Residue 219 Impacts on the Dynamics of the C-Terminal Region in Glutathione Transferase A1-1: Implications for Stability and Catalytic and Ligandin Functions†

Salerwe Mosebi, Yasien Sayed, Jonathan Burke, and Heini W. Dirr*

Protein Structure-Function Research Programme, School of Molecular and Cell Biology, University of the Witwatersrand, Johannesburg 2050, South Africa

Received September 16, 2003; Revised Manuscript Received October 31, 2003

ABSTRACT: The C-terminal region in class alpha glutathione transferases (GSTs) modulates the catalytic and nonsubstrate ligand binding functions of these enzymes. Except for mouse GST A1-1 (mGST A1-1), the structures of class alpha GSTs have a bulky aliphatic side chain topologically equivalent to Ile219 in human GST A1-1 (hGST A1-1). In mGST A1-1, the corresponding residue is an alanine. To investigate the role of Ile219 in determining the conformational dynamics of the C-terminal region in hGST A1-1, the residue was replaced by alanine. The substitution had no effect on the global structure of hGST A1-1 but did reduce the conformational stability of the C-terminal region of the protein. This region could be stabilized by ligands bound at the active site. The catalytic behavior of hGST A1-1 was significantly compromised by the I219A mutation as demonstrated by reduced enzyme activity, increased K_m for the substrates glutathione (GSH) and 1-chloro-2,4-dinitrobenzene (CDNB), and reduced catalytic efficiencies. Inhibition studies also indicated that the binding affinities for product and substrate analogues were dramatically decreased. The affinity of the mutant for GSH was, however, only slightly increased, indicating that the G-site was unaltered by the mutation. The binding affinity and stoichiometry for the anionic dye 8-anilino-1-naphthalene sulfonate (ANS) was also not significantly affected by the I219A mutation. However, the lower ΔC_p for ANS binding to the mutant (−0.34 kJ/mol per K compared with −0.84 kJ/mol per K for the wild-type protein) suggests that ANS binding to the mutant results in the burial of less hydrophobic surface area. Fluorescence data also indicates that ANS bound to the mutant is more prone to quenching by water. Overall, the data from this study, together with the structural details of the C-terminal region in mGST A1-1, show that Ile219 is an important structural determinant of the stability and dynamics of the C-terminal region of hGST A1-1.

Cytosolic glutathione transferases (GSTs; EC 2.5.1.18)[1] are a superfamily of multifunctional, dimeric enzymes grouped into numerous species-independent gene classes (for a review, see ref *1*). Each subunit has an N-terminal thioredoxin-like domain and a unique C-terminal all-helical domain (*1*−*3*). Each subunit has an independent active site comprised of a glutathione binding site (G-site) and an adjacent hydrophobic binding site for electrophilic substrates (H-site) (*4*). GSTs share a common fold, and their recognition and binding of GSH is conserved. Structural diversity at the H-site, however, distinguishes GSTs in one gene class from those in another. A structural feature that distinguishes class alpha GSTs from those of other classes is the presence of an extended C-terminal region that forms an amphipathic helix (helix 9) at the active site (*5*−*11*). The catalytic function of class alpha GST A1-1 is tightly coupled to the dynamics of the C-terminal region/helix 9 (*9*, *12*−*22*). Furthermore, hGST A1-1 is a major ligand-binding and transporter protein in the liver, capable of binding a wide variety of chemically diverse nonsubstrate compounds (*23*). Although the exact locations of ligandin sites in hGST A1-1 are unknown, recent studies indicate that nonsubstrate anionic ligands bind at or near the enzyme's active site (*24*, *25*). This would explain the inhibition of catalytic function by nonsubstrate ligands as well as the impact of the C-terminal region on the ligandin function of the protein (*9*, *12*−*18*, *26*). Thus, the catalytic and ligandin functions of hGST A1-1 can be used to monitor conformational changes in this protein region (*17*, *24*).

Hydrophobic tertiary interactions play an important role in stabilizing the C-terminal region of hGST A1-1 (*17*). Crystal structures of hGST A1-1 demonstrate the highly dynamic nature of the region that becomes localized and visible only when both G- and H-sites or the H-site are occupied by ligand (*5*, *6*, *10*). Although the conformational status of the C-terminal region in apo hGST A1-1 is unknown, the region is proposed to assume multiple open microconformational states before it is driven by ligand binding to its final, closed macroconformation (*15*, *16*, *26*,

† This work was supported by the University of the Witwatersrand, the South African National Research Foundation Grant 205359, the Wellcome Trust Grant 060799, and the Mellon Foundation.

* Corresponding author. Phone: +27 11 717 6352; fax: +27 11 717 6351; e-mail: heinid@gecko.biol.wits.ac.za.

[1] Abbreviations: ANS, 8-anilino-1-naphthalene sulfonate; CDNB, 1-chloro-2,4-dinitrobenzene; C_m, concentration of denaturant at midpoint of unfolding transition; EA, ethacrynic acid; G- and H-sites, glutathione and hydrophobic substrate binding sites; GSH, reduced glutathione; hGST A1-1, human glutathione transferase class alpha with two type-1 subunits; GSO_3^-, glutathione sulfonate; HPLC, high-performance liquid chromatography; *p*-BBGSH, *para*-bromobenzylglutathione; rmsd, root-mean-square-deviation; UV, ultraviolet.

10.1021/bi035671z CCC: $25.00
Published on Web 12/06/2003

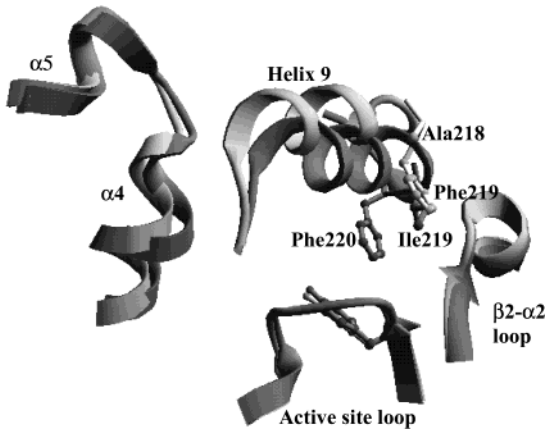

FIGURE 1: Representation of the structures of the C-terminal regions with helix 9 in human (in dark gray) (*10*) and mouse (in light gray) (*8*) GST A1-1. The side chains of Ile219 and Phe220 in hGST A1-1 and Ala218 and Phe219 in mGST A1-1 are shown in ball-and-stick. The alpha-carbons of the two proteins excluding their C-terminal regions were first superimposed (rmsd = 0.63 Å) and the representation generated with Swiss-pdb Viewer (*47*). Also shown are the positions of the active site loop with the catalytic tyrosine, the $\beta 2-\alpha 2$ loop in domain 1, and helices $\alpha 4$ and $\alpha 5$ in domain 2.

27). Two amino acid residues, Met208[2] and Phe220, contribute toward the active site and the C-terminal region's dynamics (*9*, *13*, *19*, *28*, *29*). Mutations at these positions destabilize the C-terminal region and shift the equilibrium of its conformations in apo GST A1-1 toward even more open conformations. This in turn enhances the accessibility of the G-site to GSH (*13*). The presence of a structured C-terminal region in apo hGST A1-1, albeit highly dynamic, has also been demonstrated by conformational stability studies indicating the region to unfold before the global unfolding of the protein (*17*, *30*). Binding of ligands to only the G-site of hGST A1-1 stabilizes the C-terminal region against denaturation, but the stabilizing effect is less than that afforded by GSH conjugates that induce complete closure of the C-terminal region (*5*, *6*, *10*). This is consistent with data indicating incomplete closure of the C-terminal region in rat (*9*) and human (*5*, *6*, *10*) GST A1-1 complexed with G-site ligands. On the other hand, the corresponding region in the mouse orthologue is structured and localized in its complex with GSH (*8*). Helix 9 in mGST A1-1 is, however, positionally displaced relative to that of helix 9 in hGST A1-1 giving rise to a broader H-site that is capable of accommodating larger substrates (Figure 1). A reason for these positional differences may lie in the nature of the residue at position 219 in human and rat GST A1-1 and its equivalent position (218) in mouse GST A1-1. Human and rat GSTs have a bulky isoleucine (*5*, *6*, *9*, *10*), whereas the corresponding residue in mGST A1-1 is an alanine (*8*). Ile219 is located adjacent to a key residue (Phe220) involved in modulating the conformational dynamics of the C-terminal region in human and rat GST A1-1 (*6*, *9*, *10*, *13*, *18*, *19*, *29*). The side chain of Ile219 may, therefore, play an important structural role in determining the correct positioning of the C-terminal region (and its helix 9) in human and rat GST A1-1.

[2] The amino acid residue numbering used for human class alpha GSTs includes the initiator Met as residue 1.

To investigate the role of Ile219 in determining the conformational dynamics of the C-terminal region in hGST A1-1, the residue was replaced by alanine, thus mimicking the naturally occurring mutation found in mGST A1-1. The I219A mutant was characterized in terms of its catalytic and ligandin functions, as well as the conformational stability of its C-terminal region. Data obtained from these studies, when compared to those obtained for the wild-type protein, show that Ile219 is an important structural determinant of the stability and dynamics of the C-terminal region of hGST A1-1.

EXPERIMENTAL PROCEDURES

Materials. The hGST A1-1 expression plasmid pKHA1 was a gift from Professor B. Mannervik, Uppsala University, Sweden. The restriction enzyme *Bsm*I was purchased from Roche Diagnostics Corporation, Germany. A commercial site-directed mutagenesis kit (QuikChange Site-Directed Mutagenesis kit) and mutant oligonucleotide primers were from Stratagene, USA. Ultrapure urea was from Merck, Germany. ANS, glutathione sulfonate, ethacrynic acid, and *p*-bromobenzylglutathione were from Sigma-Aldrich, USA. A site-directed mutagenesis method was used to introduce an I219A mutation into the hGST A1 coding region of the pKHA1 expression plasmid using primers designed from the published hGST A1 cDNA sequence (*31*). The following mutagenic oligonucleotide primers were used: 5′- AGAAG-CAAGGAAG***GCA***TTCAGGTTTTAAT-3′ (forward primer) and 5′- ATTAAAACCTGAATGCCTTCCTTGCTTCT-3′ (reverse primer). The underlined nucleotides denote an engineered, unique, translationally silent *Bsm*I restriction site used to screen for mutant plasmid DNA. The Ala219 codon that replaced the wild-type hGST A1 Ile219 is in bold and italicized. The I219A hGST A1 coding section of the altered pKHA1 plasmid was sequenced using a PE Applied Biosystems ABI Prism 310 genetic analyzer to ensure that no unintended mutations had been introduced during mutagenesis. Wild-type and I219A pKHA1 plasmids were transformed into *Escherichia coli* BL21 cells for expression of the GSTs. The proteins were purified by CM-Sepharose cation exchange chromatography as described (*32*). The homogeneity, molecular weights, and oligomeric status of the purified proteins were assessed by SDS/PAGE and SEC/HPLC. Protein concentrations were estimated spectrophotometrically at 280 nm using a molar extinction coefficient of 38200 M^{-1} cm^{-1} as described previously (*33*).

Enzyme Kinetics. The hGST A1-1-catalyzed conjugation of CDNB to GSH in 0.1 M sodium phosphate, 1 mM EDTA, pH 6.5 was followed spectrophotometrically at 340 nm (*34*). Steady-state kinetic parameters were determined as described (*35*). The selenium-independent peroxidase activity of hGST A1-1, which encompasses an indirect coupled reaction of GST/peroxidase with glutathione reductase (*36*), was determined by using cumene hydroperoxide as a substrate (*37*). All assays were corrected for nonenzyme rates.

Urea-Induced Equilibrium Unfolding Studies. 1 μM wild-type and I219A hGST A1-1 in 20 mM sodium phosphate buffer, pH 6.5, 1 mM EDTA, 0.1 M NaCl were unfolded at 21 °C in urea (0−8 M), as described (*30*). Urea-induced changes in the hGST A1-1 structure were monitored by intrinsic fluorescence, circular dichroism at 222 nm and

Table 1: Steady-State Kinetic Properties of Wild-Type and I219A hGST A1-1[a]

enzyme	specific activity (μmol min^{-1} mg^{-1})	K_M^{GSH} (mM)	K_M^{CDNB} (mM)	k_{cat}/K_M^{GSH} (mM^{-1} s^{-1})	k_{cat}/K_M^{CDNB} (mM^{-1} s^{-1})
wild-type	39.42 ± 0.21	0.23 ± 0.03	0.31 ± 0.01	150 ± 4	68 ± 2
I219A	10.94 ± 0.61	0.97 ± 0.04	0.78 ± 0.05	28 ± 1	24 ± 1

[a] Parameter values and their standard deviations were obtained by nonlinear regression analysis.

enzyme activity. Tryptophan fluorescence emission intensities (excitation at 295 nm) were measured at 325 and 355 nm for folded and unfolded protein, respectively.

GSH and ANS Binding. K_d values for GSH and ANS were determined for wild-type and I219A hGST A1-1 by fluorescence quenching and enhancement methods (*38*).

Determination of the pK_a for Tyr9. The ionization of Tyr9 in the active site of wild-type and I219A hGST A1-1 was measured by difference spectroscopy as described (*13*). The samples contained 20 μM GST A1-1 monomers at pH values ranging from 5.5 to 9.5, in 30 mM sodium phosphate buffer containing 30 mM glycine. Difference spectra of protein samples were recorded between 220 and 360 nm. The absorbance of the tyrosinate formed was measured at 300 nm at 20 °C. The apparent pK_a value was calculated from the peaks obtained by plotting the tyrosinate concentration per enzyme monomer, using $\Delta\epsilon_{300}$ of 2350 M^{-1} cm^{-1} (*39*) against pH.

Isothermal Titration Calorimetry. Titration experiments were conducted in a VP−ITC calorimeter from MicroCal (Northampton, MA), as described previously (*24*). Protein (0.06 mM monomer) in 20 mM sodium phosphate buffer, pH 6.5, 1 mM EDTA, 0.1 M NaCl was titrated with 5 μL increments of ANS (3.6 mM). Total observed heats of binding were corrected for heats of dilution prior to data analysis. Concentrations of protein and ANS were verified spectrophotometrically and effects due to light scattering were corrected (*40*) before data fitting. Raw data were integrated and processed with the ORIGIN 5 analysis software (MicroCal, Northampton, MA). The independent variables, K_d, ΔH, and N were obtained using the nonlinear least-squares fitting of titration curves with the ORIGIN 5 software. The free energy and entropy of binding were subsequently calculated using the following equations: $\Delta G = -RT \ln(1/K_d)$ and $\Delta G = \Delta H - T\Delta S$, where T is the absolute temperature in Kelvin.

RESULTS

Structural Characteristics of I219A hGST A1-1. Comparative structural studies with the wild-type enzyme employing tryptophan fluorescence, far-UV circular dichroism and SEC−HPLC indicated that the overall dimeric structure of hGST A1-1 was unaffected by the substitution of Ile219 with alanine (data not shown; for representative data of the wild-type hGST A1-1, see ref *41*). In fact, deletion of the entire helix 9 does not impact significantly on the structure and stability of hGST A1-1 (*17*).

Steady-State Enzyme Kinetic Properties. The specific activities of the I219A mutant with the substrates CDNB (nucleophilic substitution activity; 10.9 μmol/min per mg) and cumene hydroperoxide (selenium-independent peroxidase activity; 1.5 μmol min^{-1} mg^{-1}) are about 28 and 38%, respectively, of those for the wild-type enzyme. This and the kinetics data shown in Table 1 indicate that the I219A mutant presents a less favorable active site environment for its substrates than does the wild-type enzyme. The K_M^{GSH} and K_M^{CDNB} are increased by about 4- and 3-fold, respectively, and the k_{cat}/K_M^{GSH} and k_{cat}/K_M^{CDNB} are decreased by about 5- and 3-fold, respectively. In addition, the I219A mutant was less sensitive than the wild-type enzyme to competitive inhibition by H-site and G-site inhibitors, as indicated by their IC_{50} values in Table 2, with the greatest change seen for *p*-bromobenzylglutathione, a product analogue that occupies the G- and H-sites simultaneously. The binding of GSH to the mutant is only slightly affected (K_d = 0.25 mM for mutant and K_d = 0.18 mM for wild-type protein). These values are consistent with those (0.18−0.23 mM) reported by Widersten et al. (*42*).

Table 2: Inhibition Characteristics and Ligand Binding Constants for Wild-Type and I219A hGSTA1-1

	IC_{50} (μM)[a]			K_d (μM)[b]	
	GSO_3^-	EA	*p*-BBGSH	GSH	ANS
wild-type	6.1 ± 1.0	8.1 ± 0.3	7.5 ± 0.1	179 ± 3.6	55 ± 0.1
I219A	34.4 ± 1.0	25.5 ± 0.1	70.5 ± 1.0	247 ± 4.0	52 ± 0.5

[a] IC_{50} values are the inhibitor concentrations giving 50% inhibition at 1 mM glutathione and 1 mM 1-chloro-2,4-dinitrobenzene. [b] Determined by fluorescence methods (*38*).

Apparent pK_a of Tyr9. The ionization behavior of the hydroxyl group of the active site Tyr9 in wild-type and I219A hGST A1-1 are similar, yielding an apparent pK_a of 8.2 for both proteins (data not shown). This value is in agreement with a pK_a of 8.1 previously reported for the wild-type enzyme (*13*).

Conformational Stability Studies. Equilibrium urea-unfolding curves for I219A hGST A1-1, monitored by tryptophan fluorescence and ellipticity at 222 nm, are coincident and superimpose on those obtained for the wild-type protein (C_m = 4.5 M urea) (Figure 2). These sigmoidal curves indicate that both proteins display two-state equilibrium unfolding and share similar thermodynamic stabilities (see refs *17*, *30*, and *41*). This is not surprising given the fact that the C-terminal region does not contribute significantly toward the overall stability of the protein (*17*). However, the unfolding transitions of the wild-type protein and I219A mutant, when monitored by enzyme activity, are not coincident with their spectroscopic transitions (Figure 3A,B). Loss in enzyme activity of hGST A1-1 typically occurs at urea concentrations lower than those required for the loss of global structure due to the unfolding of the C-terminal region (*17*). However, the activity transition of the mutant occurs at even lower urea concentrations (C_m = 3.8 M) than those for the wild-type enzyme activity transition (C_m = 4.1 M). The binding of ligands to the active site (G-site for GSH, and both G- and H-sites for *p*-bromobenzylglutathione) shifts the activity transitions of both proteins toward higher urea

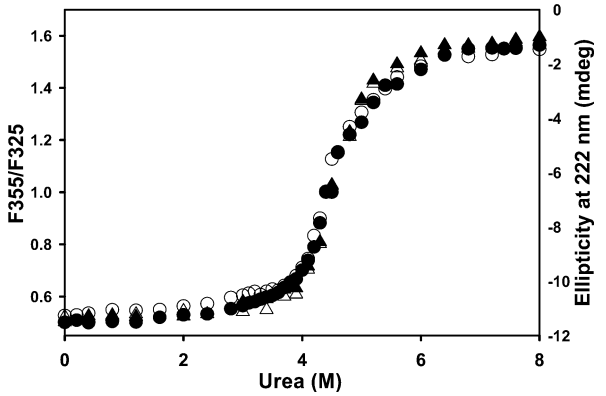

FIGURE 2: Urea-induced unfolding transitions for wild-type (filled symbol) and I219A (open symbol) hGSTA1-1 monitored with structural probes. Protein concentration is 1 μM in 20 mM sodium phosphate buffer, pH 6.5, 1 mM EDTA, 0.1 M NaCl, 0.02% sodium azide. Unfolding was monitored by measuring tryptophan fluorescence (circle) and circular dichroism at 222 nm (triangle). F355/325 is the ratio of the fluorescence intensity at 355 nm to that at 325 nm.

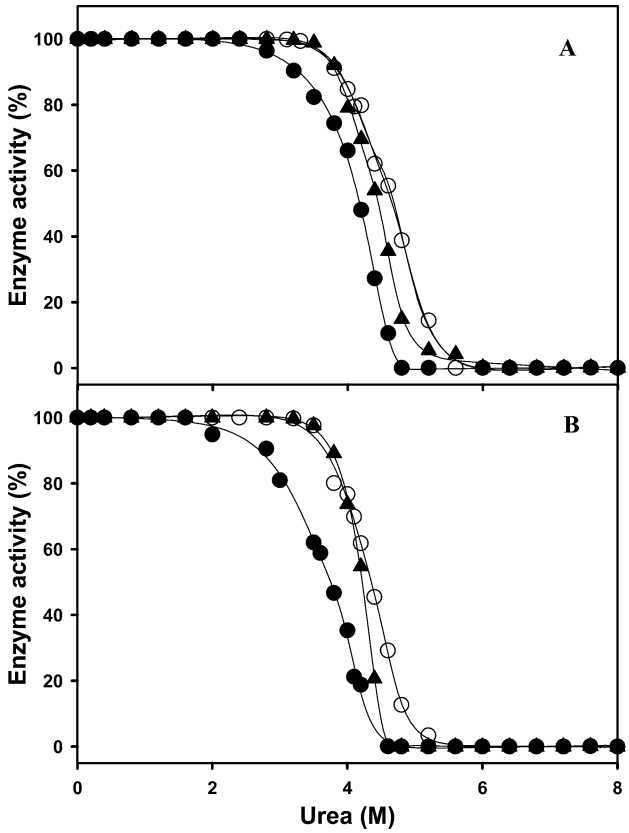

FIGURE 3: Urea-induced unfolding transitions monitored by enzyme activity of (A) wild-type and (B) I219A hGSTA1-1 in the absence (●) and presence of 10 mM glutathione (▲) and 200 μM *p*-bromobenzylglutathione (○).

concentrations (Figure 3A,B). The activity transitions in the presence of *p*-bromobenzylglutathione are coincident with the structural transitions (C_m = 4.5 M urea).

ANS Binding. Fluorescence studies indicate that ANS bound to the wild-type protein and I219A mutant emits light at the same wavelength (475 nm) but that the fluorescence intensity of ANS bound to I219A is about 35% lower than that bound to wild-type protein (data not shown; see ref *24* for similar spectra). Similar K_d values for ANS were obtained

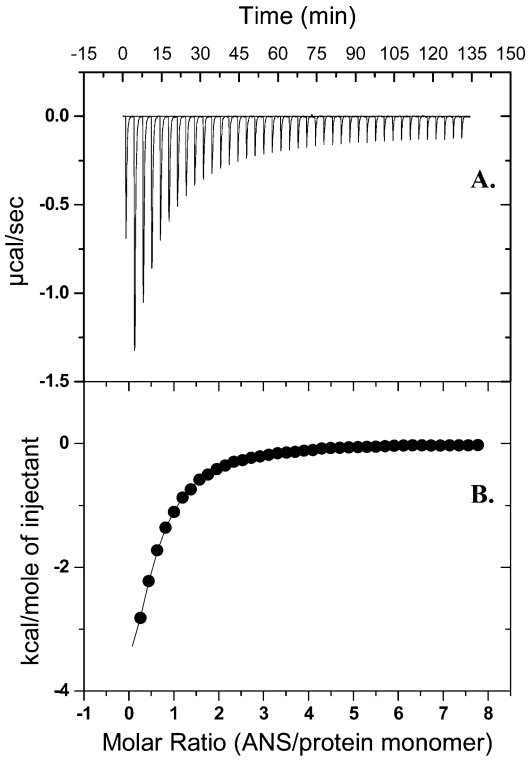

FIGURE 4: (A) Raw isothermal calorimetric titration curve of ANS binding to I219A hGST A1-1 at 10 °C in 20 mM sodium phosphate buffer, pH 6.5, containing 0.1 M NaCl, 1 mM EDTA, and 0.02% sodium azide. Protein concentration was 0.06 mM as monomer. (B) Binding isotherm of integrated data in (A) corrected for heats of dilution. The solid line through the data represents the best fit obtained using ORIGIN 5 software.

by fluorescence enhancement for wild-type and I219A hGST A1-1 (Table 2). Isothermal titration calorimetry was also used to study the binding of ANS. The raw and normalized integrated titration data for the I219A mutant shown in Figure 4 are representative of exothermic binding of the ANS anion. Like that for the wild-type protein (*24*), the integrated data for ANS binding fits best to a model based on one independent binding site per subunit. The calorimetrically determined K_d for the I219A mutant is 47 μM in agreement with that obtained from fluorescence studies, and is also similar to a K_d of 65 μM obtained for the wild-type protein (*24*). The enthalpy and entropy of binding of ANS to hGST A1-1 are temperature dependent, but, because they compensate each other, ΔG is relatively insensitive to temperature (Figure 5). ANS binding to the I219A mutant is enthalpically driven and entropically unfavorable over the temperature range studied. This unfavorable entropic effect is compensated for by the large enthalpy of binding at these temperatures. The linear temperature dependence of ΔH indicates that the heat capacity change (ΔC_p) of ANS binding is independent of temperature within the experimental temperature range. The magnitude of ΔC_p for ANS binding to the mutant is −0.34 kJ/mol per K compared with −0.84 kJ/mol per K for the wild-type protein (*24*).

DISCUSSION

The I219A substitution in the C-terminal region of hGST A1-1 does not alter the global structure or conformational stability of the protein. These results are in agreement with previous findings for the C-terminal deletion mutant of hGST

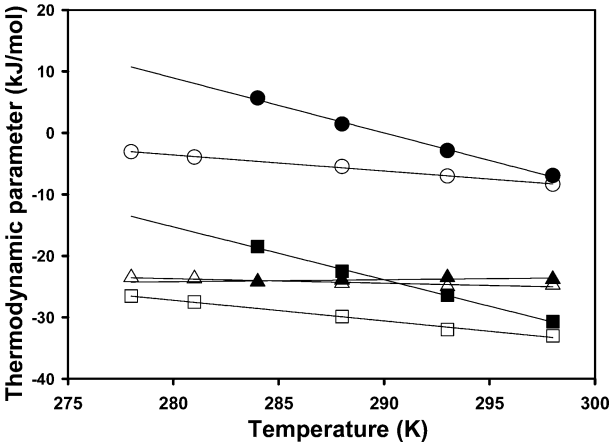

FIGURE 5: Temperature dependence of the thermodynamic parameters for the binding of ANS to wild-type (filled symbols) and I219A hGST A1-1 (open symbols). Key: Triangles, blocks, and circles represent ΔG, ΔH, and $T\Delta S$ values, respectively. The solid lines were obtained by linear regression analysis of each set of data.

A1-1 (*17*). The catalytic function of the I219A hGST A1-1 mutant is, however, significantly altered relative to the wild-type protein. This is reflected by its reduced nucleophilic substitution (with GSH and CDNB) and selenium-independent peroxidase (with GSH and cumene hydroperoxide) activities, reduced catalytic efficiencies for GSH and CDNB, and enhanced K_m values for GSH and CDNB. The binding affinities for G- and H-site competitive inhibitors were also diminished with the greatest reduction observed for *p*-bromobenzylglutathione, a compound that simultaneously binds the G- and H-sites (*5*).

Although the stability of the core GST structure was unaffected by the I219A mutation, the spectroscopic probes used are insensitive to structural changes in the C-terminal region. Enzyme activity, however, is a sensitive probe that can be used to monitor conformational changes in this region of the class alpha GST (*17*, *30*, *41*). The shift observed in the activity-unfolding transition of I219A hGST A1-1 to lower urea concentrations (C_m = 3.8 M urea compared to 4.1 M urea for wild-type protein), demonstrates that the region is destabilized by the mutation. The region's stability was, however, enhanced when GSH binds to the G-site (C_m shifts to 4.1 M urea) or when *p*-bromobenzylglutathione binds to both the G- and H-sites (C_m shifts to 4.5 M urea). The greater stabilizing effect exerted by *p*-bromobenzylglutathione is consistent with an increased formation of tertiary interactions between the C-terminal region and the protein when complexed with GSH conjugates (*17*). Since the C-terminal region in apo human and rat GST A1-1 is too dynamic to be observed by X-ray diffraction (*6*, *9*, *10*), its conformational status in the absence of active site ligands is unclear. Rather than being completely disordered (*15*, *16*), the C-terminal region is most likely structured but delocalized near the surface of the apo protein (*13*, *17*). Mutations at positions 208 and 220 have also been shown to destabilize the region resulting in increased accessibility of the active site (*13*). That tertiary interactions play an important role in the folding of the C-terminal region, which is consistent with the proposal that its structuring occurs only after the folding and assembly of the dimeric structure (*17*).

Given the tight coupling between the dynamics of the C-terminal region and the catalytic function of GST A1-1 (*12*, *13*, *15*, *16*, *18*−*21*), an explanation for the altered catalytic function of I219A hGST A1-1 should lie in the dynamic nature of the C-terminal region in this protein. In the absence of structural details for I219A GST A1-1, clues about the possible conformation of the C-terminal region in this protein can be gained from the crystal structures of murine GST A1-1 complexed with GSH or glutathione conjugate of (+)-anti-7,8-dihydroxy-9,10-oxy-7,8,9,10-tetrahydrobenzo-[*a*]pyrene (*8*). The murine and human GST A1-1 structures, excluding their C-terminal regions/helix 9, are similar (rmsd = 0.63Å), and their GSH moieties bind the same positions in the proteins and have similar conformations. Although helix 9 in these structures is similar in sequence and length, helix 9 is positionally displaced in mGST A1-1 relative to helix 9 in ligand-complexed hGST A1-1 (Figure 1). The reason for these positional differences may lie in the nature of the residue at position 218 in mGST A1-1 and its equivalent position (219) in hGST A1-1. In the murine protein, residue 218 is an alanine, thus representing a natural I219A mutant of the human orthologue. A bulky aliphatic side chain corresponding to Ile219 in hGST A1-1 is also found in the structures of rat GST A1-1 (*9*) and murine (*43*) and human A4-4 GSTs (*7*). Due to the absence of a bulky side chain at position 218 in mGST A1-1, helix 9 is rotated and the phenyl side chain of Phe219 occupies a space over domain I that is equivalent to the space occupied by Ile219 in the human protein (Figure 1). The longer phenyl side chain of Phe219 elevates helix 9, thus creating a space between the helix and domain I. These positional displacements in helix 9 result in far fewer contacts between helix 9 and the rest of mGST A1-1, which, together with the absence of the phenyl side chain of Phe219 at its normal topological position in the structures of ligand-complexed hGST A1-1, give rise to a less constricted active site. In the murine and human structures, Phe219 and Ile219 pack against hydrophobic walls formed by residues in the β2-α2 loop of domain I (Phe9, Gln35, Ser36, Pro37 for mGST A1-1 and Phe10, Ala12, Ile35, Lys36, Ser37, Ala38, Leu41 for hGST A1-1). This loop region, together with the C-terminal region of helix 4 (Val109, Leu110 in mGST A1-1, and Pro110 and Val111 in hGST A1-1) in domain II, most likely restricts the lateral movement of helix 9 across the surface of domain I. The salt bridge between Arg221 and Asp42 might not play a significant role in positioning helix 9 in hGST A1-1, since it is not conserved in all the structures of GST A1-1 complexed with various ligands (*5*, *6*). The equivalent salt bridge is also not present in mGST A1-1.

In light of the above, it seems feasible that the I219A mutation results in a positional displacement of the C-terminal region in hGST A-1 having fewer interactions with the protein and, thus, diminished stability. The displacement would also result in a reduction in catalytic function. Phe220 mutants of hGST A1-1 are also suggested to possess a displaced, open C-terminal region that results in diminished activities and catalytic efficiencies, and a more accessible G-site (*13*). The C-terminal region in human and rat GST A1-1 contributes more significantly toward the H-site than toward the G-site. Deletion of this region appears not to impact much on the binding of GSH to the G-site than it does on the binding of ligands to the H-site (*12*, *17*). A positional displacement of the C-terminal region, induced by the I219A mutation should, therefore, have a greater

impact on the binding of ligands to the H-site. This is consistent with our data indicating that the mutation does not affect GSH binding but significantly affects the binding of EA and *p*-bromobenzylglutathione. The reason for the reduced affinity for GSO_3^-, a G-site ligand, is not clear. It is unlikely that this is due to a lowering in the apparent pK_a of Tyr9 since a value of 8.2 was obtained for both wild-type and mutant proteins. A displaced C-terminal region in hGST A1-1 has been shown to maintain the unusually low pK_a of this active site tyrosine (*13*).

hGST A1-1 is also a major ligand-binding protein, known historically as ligandin, in the liver, capable of binding a wide range of chemically diverse nonsubstrate compounds (*23*). Although the ligandin function of the protein does not involve catalysis, the binding of nonsubstrate ligands can inhibit catalytic function. Due to the absence of crystal structures of hGST A1-1 complexed with nonsubstrate ligands, the location of the ligandin site(s) remains uncertain. Clues about its location within the cleft between the two subunits or at a site distinct from both the G- and the H-sites but near the active site, have been provided by affinity labeling studies on rat GST A1-1 (*44*). The anionic ligand ANS binds the wild-type and I219A mutant hGST A1-1 with a stoichiometry of two molecules of ANS per dimer (*24*, this study). We have shown that ANS binds at/near the H-site (*24*) and that the binding of the anionic dye can be used to monitor conformational changes in the C-terminal region (*17*). The location of the ANS binding site is in agreement with the findings of a recent kinetics study with hGST A1-1 indicating that lithocholate and oestradiol disulfate act as H-site competitive rather than noncompetitive inhibitors, suggesting that these nonsubstrate anionic ligands also bind at or near the H-site (*25*). The anionic nonsubstrates bromosulfophthalein and cibacron blue have also been shown to bind the H-site in crystal structures of hGST P1-1 (*45*). Given the impact that the I219A mutation in hGST A1-1 has on ANS binding (altered fluorescence intensity and ΔC_p), the conformation of the C-terminal region in the mutant appears not to be the same as that in the wild-type enzyme (see discussion above). The linearity in the ΔC_p determination excludes the possibility of thermal effects on the conformation of the C-terminal region within the experimental temperature range (this study, *24*). Although the ANS binding data indicate that the affinity of hGST A1-1 for the anionic dye is not altered significantly by the I219A mutation, the heat capacity of binding is increased from −0.84 kJ/mol per K (wild-type protein) to −0.34 kJ/mol per K (mutant). Since negative ΔC_p values are expected for the burial of solvent exposed, nonpolar surfaces (*46*), the above ΔC_p values for hGST A1-1 indicate a reduction in the hydrophobic component in the mutant protein−ANS interaction. The ANS binding site in hGST A1-1 is not anhydrous (*24*). The reduced fluorescence intensity of ANS bound to the I219A mutant, when compared with that for the wild-type protein, suggests that the dye is more prone to quenching by water.

REFERENCES

1. Sheehan, D., Meade, G., Foley, V. M., and Dowd, C. A. (2001) *Biochem. J. 360*, 1−16.
2. Dirr, H. W., Reinemer, P., and Huber, R. (1994) *Eur. J. Biochem. 220*, 645−649.
3. Armstrong, R. N. (1997) Structure, catalytic mechanism, and evolution of the glutathione transferases. *Chem. Res. Toxicol. 10*, 2−18.
4. Mannervik, B. (1985) *Adv. Enzymol. Relat. Areas Mol. Biol. 57*, 357−417.
5. Sinning, I., Kleywegt, G. J., Cowan, S. W., Reinemer, P., Dirr, H. W., Huber, R., Gilliland, G. L., Armstrong, R. N., Ji, X., Board, P. G., Olin, B., Mannervik, B., and Jones, T. A. (1993) *J. Mol. Biol. 232*, 192−212.
6. Cameron, A., Sinning, I., L'Hermite, G., Olin, B., Board, P., Mannervik, B., and Jones, T. (1995) *Structure 3*, 717−727.
7. Bruns, C. M., Hubatsch, I., Ridderstrom, M., Mannervik, B., and Tainer, J. A. (1999) *J. Mol. Biol. 288*, 427−439.
8. Gu, Y., Singh, S., and Ji, X. (2000) *Biochemistry 39*, 12552−12557.
9. Adman, E. T., Le Trong, I., Stenkamp, R. E., Nieslanik, I., Dietze, E. C., Tai, G., Ibarra, C., and Atkins, W. M. (2001) *Proteins: Struct., Funct., Genet. 42*, 192−200.
10. Le Trong, I., Stenkamp, R. E., Ibarra, C, Atkins, W. M., and Adman, E. L. (2002) *Proteins: Struct., Funct., Genet. 48*, 618−627.
11. Gu, Y., Xiao, B., Wargo, H. L., Bucher, M. H., Singh, S. V., and Ji, X. (2003) *Biochemistry 42*, 917−923.
12. Board, P. G., and Mannervik, B. (1991) *Biochem. J. 275*, 171−174.
13. Gustafsson, A., Etahadieh, M., Jemth, P., and Mannervik, B. (1999) *Biochemistry 38*, 16268−16275.
14. Allardyce, C. S., McDonagh, P. D., Lian, L. Y., Wolf, C. R., and Roberts, G. C. (1999) *Biochem. J. 343*, 525−531.
15. Nieslanik, B., Dabrowski, M. J., Lyon, R. P., and Atkins, W. M. (1999) *Biochemistry 38*, 6971−6980.
16. Nieslanik, B., Dietze, E. C., Atkins, W., Trong, I., and Adman, E. T. (1999) *Pac. Symp. Biocomput*. 554−565.
17. Dirr, H. W., and Wallace, L. A. (1999) *Biochemistry 38*, 15631−15640.
18. Ibarra, C., Nieslanik, B. S., and Atkins, W. M. (2001) *Biochemistry 40*, 10614−10624.
19. Nilsson, L. O., Edalat, M., Pettersson, P. L., and Mannervik, B. (2002) *Biochim. Biophys. Acta 1597*, 157−163.
20. Nieslanik, B., and Atkins, W. M. (2000) *J. Biol. Chem. 275*, 17447−17451.
21. Allardyce, C. S., McDonagh, P. D., Prescott, A., Roberts, G. C. K., and Lian, L. Y. (2000) *Clin. Chem., Enzymol. Commun. 8*, 239−253.
22. Ibarra, C. A., Chowdhury, P., Petrich, J. W., and Atkins, W. M. (2003) *J. Biol. Chem. 278*, 19257−65.
23. Listowsky, I. (1993) Glutathione S-transferases: intracellular binding, detoxification and adaptive responses in *Hepatic Transport and Bile Secretion: Physiology and Pathophysiology* (Tavoloni, N., and Berk, P. D., Eds.) pp 397−403, Raven Press, New York.
24. Sayed, S., Hornby, J. A. T., Lopez, M., and Dirr, H. (2002) *Biochem. J. 363*, 341−346.
25. Lyon, R. P., and Atkins, W. M. (2002) *Biochemistry 41*, 10920−10927.
26. Nieslanik, B., Ibarra, C., and Atkins, W. M. (2001) *Biochemistry 40*, 3536−3543.
27. Lian, L. Y. (1998) *Cell. Mol. Life Sci. 54*, 359−362.
28. Widersten, M., Bjornestedt, R., and Mannervik, B. (1994) *Biochemistry 33*, 11717−11723.
29. Atkins, W. M., Dietze, E. C., and Ibarra, C. (1997) *Protein Sci. 6*, 873−879.
30. Wallace, L. A., Sluis-Cremer, N., and Dirr, H. W. (1998) *Biochemistry 37*, 5320−5328.
31. Stenberg, G., Bjornestedt, R., and Mannervik, B (1992) *Protein Expr. Purif. 3*, 80−84.
32. Sayed, S., Wallace, L. A., and Dirr, H. W. (2000) *FEBS Lett. 465*, 169−172.
33. Perkins, S. (1986) *Eur. J. Biochem. 157*, 169−180.
34. Habig, W. H., and Jakoby, W. B. (1981) *Methods Enzymol. 77*, 398−405.
35. Gustafsson, A., and Mannervik, B. (1999) *J. Mol. Biol. 288*, 787−800.
36. Ahmad, S., Pritsos, C. A., Bowen, S. M., Heisler, C. R., Blomquist, R. S., and Pardini, R. S. (1988) *Free Radical Res. Commun. 4*, 403−408.
37. Stenberg, G., Board, P. G., and Mannervik, B. (1991) *FEBS Lett. 293*, 153−155.

38. Bico, P., Erhardt, J., Kaplan, W., and Dirr, H. (1995) *Biochim. Biophys. Acta 1247*, 225−230.
39. Bjornestedt, R., Stenberg, G., Widersten, M., Board, P. G., Sinning, I., Jones, T. A., and Mannervik, B. (1995) *J. Mol. Biol. 247*, 765−773.
40. Winder, A. F., and Gent, W. L. (1971) *Biopolymers 10*, 1243−1251.
41. Wallace, L. A., Blatch, G. L., and Dirr, H. W. (1998) *Biochem. J. 336*, 413−418.
42. Widersten, M., Bjornestedt, R., and Mannervik, B. (1996) *Biochemistry 35*, 7731−7742.
43. Krengel, U., Schroter, K. H., Hoier, H., Arkema, A., Kalk, K. H., Zimniak, P., and Dijkstra, B. W. (1998) *FEBS Lett. 422*, 285−290.
44. Barycki, J. J., and Colman, R. F. (1997) *Arch. Biochem. Biophys. 345*, 16−31.
45. Oakley, A. J., Lo, B. M., Nuccetelli, M., Mazzetti, A. P., and Parker, M. W. (1999) *J. Mol. Biol. 291*, 913−926.
46. Loladze, V. V., Ermolenko, D. N., and Makhatadze, G. I. (2001) *Protein Sci. 10*, 1343−1352.
47. Guex, N., and Peitsch, M. C. (1997) *Electrophoresis 18*, 2714−2723.

BI035671Z